Prokaryotic microbiota outperform eukaryotic microbiota in differentiating between infection states of iconic diseases of two commercial oyster species

Wegner K. Mathias [1, *], Morga Benjamin [2], Guillou Laure [3], Strittmatter Martina [3], Lecadet Cyrielle [2], Travers Marie-Agnes [2, 4], Tourbiez Delphine [2], Gervais Ophelie [2], Arzul Isabelle [2]

[1] Alfred Wegener Institute (AWI) - Helmholtz Centre for Polar and Marine Research, Coastal Ecology, Wadden Sea Station Sylt, Hafenstrasse 43, 25992 List, Germany
[2] Ifremer, ASIM Adaptation et Santé des Invertébrés Marins, F-17390 La Tremblade, France
[3] Sorbonne Université, CNRS, Adaptation and Diversity in Marine Environment (UMR7144), Ecology of Marine Plankton (ECOMAP Team), Station Biologique de Roscoff, 29680 Roscoff, France
[4] IHPE, Univ Montpellier, CNRS, IFREMER, Univ Perpignan Via Domitia, Montpellier, France

* Corresponding author : Mathias K. Wegner, email address : mathias.wegner@awi.de

Abstract :

The role of microbiota in health and disease is most often expressed by structural shifts of the taxonomic composition of prokaryote communities in infected and healthy individuals. In cultured aquatic animals with open circulatory systems, such as mollusks, microbiota also harbor a wide range of protists, which are unicellular eukaryotes that could also play an important role during infections. To evaluate the effectiveness of eukaryotic vs. prokaryotic microbiota in characterizing infection states, we examined both microbial compartments under natural conditions in two commercially important oyster species, the flat oyster Ostrea edulis and the Pacific oyster Magallana (Crassostrea) gigas. With O. edulis being infected by two protist parasites, Marteilia refringens and Bonamia ostreae, and M. gigas being infected by the ostreid herpes virus OsHV-1, we chose iconic diseases responsible for substantial mortalities and economic damage within the two species. We analyzed and compared the structural and compositional differences between healthy and infected oysters and used random forest machine learning to classify infection states and identify indicator taxa that distinguish healthy from infected individuals. Both at the structural and compositional levels, bacterial microbiota proved to be better predictors of infection states. By eliminating noisy taxa through variable selection in the random forest models, we enhanced the compositional differences between infection states. In all host-pathogen combinations, only a few taxa (<31) were required to achieve optimal separation. While the identity of indicator taxa will partly reflect the specific environmental conditions at the time of sampling, we recovered several previously described indicator taxa, such as Mycoplasma, Vibrio, Photobacterium, and Arcobacter. Next to these we also discovered new taxa like Motiliproteus that exhibited the potential to differentiate between infection states of the investigated O. edulis specimen. The simultaneous characterization of prokaryotic and eukaryotic microbiota suggests that only few prokaryotic indicator species might be needed to reliably differentiate between infected from healthy individuals and monitor infection risks.

Highlights

► Bacterial microbiota are more strongly associated to infection states than protist microbiota. ► Only few indicator taxa are needed to maximize differentiation between infection states. ► The higher information content of only a few bacterial taxa needed to identify disease states was found across three pathogens and two commercially important oyster hosts.

1 Introduction

The marine environment is rich in microbial life (Whitman et al., 1998), with viruses, prokaryotes (bacteria, archaea) and eukaryotes exhibiting high structural and functional diversity (Sunagawa et al., 2015). Many microbes exist in association with other organisms, forming individually-based biocenosis known as meta-organisms or holobionts (Desriac et al., 2014; Esser et al., 2019). Marine bivalves, in particular, are exposed to a plethora of microbes due to their filter-feeding lifestyle and open circulatory system. The bacterial microbiota of bivalves play a significant role in nutrition and physiology of the host as well as in various biogeochemical processes contributing to nutrient cycling and bentho-pellagic coupling (Ray and Fulweiler, 2020). While much research on mollusks has focused on the prokaryotic diversity in relation to disease (Paillard et al., 2022), it is essential to recognize that bivalve tissues are complex systems consisting of multiple microbiome compartments comprising viral, bacterial and eukaryotic microbiota (Dupont et al., 2020). There is a pressing need for studies exploring non-bacterial microbiome compartments (Dupont et al., 2020), as all microbiome compartments are interconnected and not independent of one another. For instance, viral infections can influence the pathogenicity of prokaryote communities (de Lorgeril et al., 2018), while eukaryotic microbiota can impact prokaryote microbiota and vice versa (Chabe et al., 2017; Even et al., 2021). Indeed, there is a lack of specific examples from marine bivalves that illustrate how eukaryotes and prokaryotes form compartment-specific functional responses to infection. Given that changes in community composition can impact the health and fitness of the host, it is likely that the various microbiota compartments also fulfil different functions for the host, particularly in terms of host immunity (King et al., 2019b).

Until now, the impact of infection on mollusk microbiomes has often been described in terms of overall structural differences in the community, encompassing bacterial diversity within (alpha-diversity) and between individuals (beta-diversity (Paillard et al., 2022)). Infection-related dysbiosis has frequently

been associated with reduced alpha (Clerissi et al., 2020a; Portet et al., 2021) and increased beta diversity (de Lorgeril et al., 2018; Lokmer and Wegner, 2015). However, it can be reasonably assumed that not all symbiotic microbes contribute equally to disease susceptibility, resistance, or modulation of pathogen virulence. Only a limited number of studies have attempted to identify specific causative taxa by focusing on the most common or core taxa. This knowledge is crucial for distinguishing beneficial microbes (e.g. probiotics; Desriac et al., 2014; Kesarcodi-Watson et al., 2012) from harmful ones (the pathobiome Bass et al., 2019).

Environmental changes can lead to significant fluctuations in microbial communities (Wegner et al., 2013), thereby reducing the number of core microbiota shared by many individuals over time to just a few taxa (Lokmer, A. et al., 2016). In addition, pathogens typically target specific tissues, which can vary between different infectious agents (Holmes, 1973). The considerable diversity between tissues (Lokmer, Ana et al., 2016) further complicates the identification of beneficial or harmful microbes. Therefore, it is a challenging task to single out meaningful taxa from such dynamic and highly diverse communities, akin to finding a needle-in-a-haystack. Statistical approaches often face the issue of overfitting, where the number of taxa used as parameters exceeds the available number of samples (Broadhurst and Kell, 2006). To address this challenge, classification algorithms based on machine learning techniques have proven to be effective in reducing over-parameterization. Specifically, models utilizing random forest classification have been successfully applied in the classification of microbiome data (Statnikov et al., 2013), including studies related to oyster disease (Delisle et al., 2022).

Here, we employ machine learning algorithms to classify infection states and identify microbial taxa from the tissue-specific bacterial and protist compartments associated with well-known diseases in oysters: *Marteilia refringens* and *Bonamia ostreae* infections in European flat oysters (*Ostrea edulis*) and ostreid herpes virus (OsHV-1) infection in Pacific oysters (*Magallana* (*Crassostrea) gigas*).

Marteilia refringens and Bonamia ostreae are protozoan parasites belonging to Ascetosporea. Initially detected during mortality events in Brittany, France, in the 1970s and 1980s, these parasites subsequently spread to other oyster farming areas through the transfer of infected oysters (Arzul et al., 2006). Infections caused by *M. refringens* and *B. ostreae* have significantly contributed to the decline of the flat oyster populations in France(Pouvreau et al., 2021; Pouvreau et al., 2023). Due to its economic and ecological importance, the flat oyster is currently the focus of various restoration initiatives across Europe (https://noraeurope.eu/). Understanding the response of *O. edulis* and its microbiota to pathogen infections can therefore greatly contribute to the success of these restoration efforts.

Previous studies have demonstrated that infection with *Marteilia* species can alter the bacterial microbiome in Sydney rock oysters (*Saccostrea glomerata*; (Green and Barnes, 2010; Nguyen et al., 2021). However, further investigations are necessary to identify common trends in the association between microbiota and protist infections in bivalves.

Ostreid herpesvirus type 1 (OsHV-1) is the primary cause of a disease that leads to significant economic losses in the global Pacific oyster industry. It is one of the two known members of the Malacoherpesviridae family (Bai et al., 2021). OsHV-1 is a large enveloped virus capable of infecting several bivalve species, including *Ostrea edulis*, *Pecten maximus*, and *Ruditapes philippinarum* (Arzul et al., 2017; Arzul et al., 2001). In 2008, a highly virulent variant of OsHV-1, known as OsHV-1 µVar, emerged in France (Segarra et al., 2010). Given the global impact of OsHV-1, there is an urgent need to gain a better understanding of the disease and propose measures for controlling OsHV-1 infections. This included studying the bacterial (de Lorgeril et al., 2018) and protist (Dupont et al., 2020) compartments of the oyster-associated microbiota. To the best of our knowledge, no study has yet attempted to evaluate the relative role of different microbiota compartments across a range of diseases in different host species. However, such integrative studies are necessary to assess the generalizability of the observed patterns.

To capture these associations between oyster microbiota and natural diversity under field conditions, we characterized the prokaryotic and eukaryotic microbial communities in different body compartments of wild-caught oysters that were naturally infected. To ensure that we focused on active microbes, we utilized reversed transcribed RNA. We separated the prokaryotic and eukaryotic microbial communities and grouped individuals into different qualitative infection states (infected by *M. refringens* or *B. ostreae* for *O. edulis* and infected by OsHv-1 for *M. gigas*) based on Real-Time PCR results. Subsequently, we classified individual infection states based on their pro- and eukaryotic microbiota using random forest machine learning. The discriminative capabilities of these models represent an initial step towards identifying relevant taxa characterising infected individuals. This knowledge can contribute to our understanding of the relative importance of different microbiome compartments in health and disease under natural conditions.

2 Material & methods

2.1 Collection of biological material

Adult flat oysters (*Ostrea edulis*) were sampled by diving in Daoulas Bay, Rade de Brest (Finistère, France) during four periods in 2016. The purpose was to maximize the likehood of obtaining oysters with varying levels of infection from both *Bonamia ostreae* and *Marteilia refringens* (Table 1). It is important to note that no mortality event of flat oyster was reported in Rade de Brest during the study period. *Magallana (Crassostrea) gigas* spat, on the other hand, were initially gathered from Fouras, Charente Maritime, France, and were subsequently placed on oyster tables in La Floride, Marennes-Oléron (Charente-Maritime; France) starting from March 2016. To assess the impact of disease on the oyster microbiota, sampling was conducted both before, during, and after a mortality outbreak

associated with OsHV-1 (Table 1). Notably, a mortality outbreak, resulting in a mortality of 60-70%, was detected in the period around May 24th, 2016.

After collecting 30 oysters per sampling time point, the oysters were kept and transported without water at 4°C and processed immediately at reception. Four different types of body compartments were used for microbiome analyses: pallial fluid, hemolymph, gill, and digestive gland. To collect pallial fluid, a hole was drilled into the shell, which was then disinfected with bleach and rinsed with sterile water, and the fluid was extracted using a sterile syringe. Hemolymph was extracted from the adductor muscle by administering a sterile syringe through a notch in the edge of the shell, providing access to the muscle.

After collecting the fluids, the oysters were shucked, and sterile scissors were used to cut a ~50mg piece of gill and digestive gland tissue. All samples were flash frozen and stored at -80° C prior to nucleic acid extraction.

Table 1. Details of the sampling dates, infection state, and sequencing of the oyster material used. The number of libraries that passed quality critieria and were sequenced in sufficient depth is specified for each tissue in the prokaryotic and eukaryotic microbiota. HL = hemolymph, PF = pallial fluid, G = gill, DG = digestive gland. * Mortalities of 60-70% were observed in the period around 24/05/2016. ** Results based on Real Time PCR analyses

Species	Date	# of specimen Libraries analyzed: 16s (HL, PF, G, DG) 18s (HL, PF, G, DG)	Infection rates %** in sequenced samples		
			Bonamia	*Marteilia*	Total
O. edulis	01/03/2016	12 38 (12,12,8,6) 43 (11,11,10,11)	42%	0%	42%
	29/04/2016	11 37 (11,11,10,5) 27 (7,5,7,8)	18%	36%	54%
	30/06/2016	12 44 (11,12,12,9) 40 (11,11,8,10)	0%	50%	50%
	30/09/2016	12 46 (11,12,11,12) 38 (11,11,10,5)	8 %	50%	58%
M. gigas			*OsHV-1 positive*		
	15/03/2016	12 46 (12,11,11,12) 45 (11,12,12,10)	50%		
	25/05/2016*	12 45 (10,11,12,12) 40 (12,12,11,12)	50%		

04/10/2016	Not sequenced	0%

2.2 Nucleic Acid isolation and sequencing

DNA and RNA were extracted simultaneously from the same body compartment sample using the

Qiagen AllPrep RNA/DNA kit (Strittmatter, 2023b). The infection state of the oysters was determined

by quantitatively measuring the amount of pathogen DNA using real-time PCR. For flat oysters, the

DNA fraction obtained from gill and digestive gland tissue was used, while for the Pacific oysters, gill

tissue was used (Canier et al., 2020; eurl-mollusc.eu, 2023). *O. edulis* were considered infected if the Ct

values for *Bonamia ostreae* and *Marteilia refringens* PCRs were smaller than 38 (Canier et al. 2020). With

these analyses we could differentiate between three qualitative infection states in *O. edulis*:

"uninfected", "infected by *B. ostreae*", and "infected by *M. refringens*". *M.gigas* oysters were considered

infected if the Ct values for OsHV-1 PCR were smaller than 32, resulting in two infection states:

"uninfected" and "infected by OsHv-1" (eurl-mollusc.eu, 2023). To ensure a balanced representation of

infected and uninfected samples, only sampling time points with detected infections were used, and up

to 12 samples per time point were chosen for sequencing of all four body compartments (Table 1). It

should be noted that the oyster microbiota vary significantly, with only a few taxa persisting over time

(Lokmer, A. et al., 2016). To remove the temporal signature and identify infection states, samples from

different sampling time points were included in a pooled analysis. For *O. edulis*, all four time points

were used for sequencing, aiming to achieve an overall infection rate of approximately 50% for each

time point to maximize statistical power. The observed infection frequencies within the 47 analyzed

oyster samples ranged from 42 to 58%, but differed between the two parasites (Table 1).

For *M. gigas*, 24 individuals were selected from the two time points where infected oysters were found

for microbiome analyses. For each sampling date 6 infected and 6 uninfected oysters were used to

generate a balanced sampling design. The RNA fraction of the nucleic acid isolation was used for

microbiome metabarcoding to capture only active microbiota. The RNA was reverse transcribed into

cDNA using random hexamer primers. 16srRNA amplicon sequencing of the V3-V4 region was conducted using the Earth microbiome primers (Parada 515F GTGYCAGCMGCCGCGGTAA and Apprill 806R GGACTACNVGGGTWTCTAAT), and 18srRNA was amplified using the 18SV1V2 primers (forward ACCTGGTTGATCCTGCCA and reverse GTARKCCWMTAYMYTACC) (Clerissi et al., 2020b) on the cDNA fractions (Strittmatter, 2023a).

The PCR products were pooled in equimolar amounts, and sequencing libraries of these pools were constructed and sequenced on the Illumina MiSeq platform following the manufacturer's specifications. Within each run, Amplicon Sequence Variants (ASVs) were identified from demultiplexed reads using the dada2 pipeline (Callahan et al., 2016) with the parameters maxN = 0, maxEE= 2,10, truncQ = 2. Adapters were trimmed, and sequences were cut to a length of 253 bp for 16srRNA and 340 bp for 18srRNA. Chimeric sequences were removed, and all runs were merged into one Phyloseq dataset containing the ASV-table, taxonomy, sequences, and metadata. To discriminate bacterial from eukaryotic ASVs, bacterial ASVs are shown with capital letters (i.e. ASV0000) and eukaryotes in small print (i.e. asv0000). Sequencing data and associated metadata are available as short reads archived in the bioproject PRJNA1041076.

2.3 Data analyses

Since our focus was not to reveal differences between species, we analyzed European flat oyster samples separately from Pacific oyster samples. Initially, we filtered out singletons and taxa that occurred in only one sample. Further filtering of taxa was based on the observed empirical distribution of ASV relative abundance. To achieve this, we removed taxa from the rare tail of the distribution, where the overall relative abundance was smaller than the mode of the ASV relative abundance distribution (see supplemental Fig. 1 for specific cut-off values in each data set). Considering the observed saturation of rarefaction curves, we rarified all

samples to 10,000 reads. We identified only one *O. edulis* specimen that was infected by both

parasites and removed this individual from the analysis. In order to exclude the influence of

both eukaryotic parasites on the analyses of eukaryotic communities, we removed all taxa with

a genus affiliation to either *Bonamia* or *Marteilia*, as well as taxa identified as *Ostrea*, which

represent host contamination.

2.3.1 Alpha diversity

Generalized linear mixed models (GLMM) were fitted to determine the effect of body

compartment and infection state on the number of ASVs (richness) and Shannon's diversity

index. Individual oyster identity was fitted as random intercept to account for body

compartments originating from the same individual. Results were summarized by Type III

Wald chi-square analysis of deviance. If a significant tissue * infection interaction term was

observed, we further investigated the effect of infection in individual body compartments by

fitting separate linear models for each body compartment. We then tested for differences in

diversity measures between infection states using uninfected individuals as a reference.

2.3.2 Infection state classification

Taxa that helped the classification of infection state were identified using a multiclass random

forest machine learning approach. Random forest classification is a flexible classification

algorithm that avoids overfitting by using majority voting to combine predictions from many

decision trees into a more accurate and robust overall model. For each microbiome

compartment per oyster species we generated training and test data sets by randomly splitting

the full data set in a 3:1 ratio maintaining the original ratio between infected and uninfected individuals. To tune the hyper-parameters of the decision trees, we employed k-fold cross-validation and randomly divided the data into five folds. We used the first fold as a validation set, and the remaining four folds for fitting the model. Hyperparameters included the number of trees used for majority voting (100 trees), number of features/variables and minimum tree depth. The random forest classification process was repeated with 20 random splits, and the model with the highest classification accuracy on the full dataset was selected as the best random forest model (best RF). To identify the taxa that contributed overproportionally to the differentiation between infected and uninfected individuals, we examined the taxa that had the highest variable importance (top 99th percentile) in the best random forest model.

2.3.3 Beta diversity

Beta diversity, i.e. the differences in community composition between individuals, was analysed using permutational multivariate analysis of variance (PERMANOVA) based on pairwise Bray-Curtis distances using the *adonis* function of the vegan package. Body compartment, infection state, and their interaction term were fitted as independent variables. To validate the effectiveness of the taxa identified by the random forest classification in distinguishing between infected and uninfected individuals, PERMANOVA analyses were conducted using hierarchically structured datasets. Initially, the full dataset consisting of all ASVs that passed the initial filtering steps was used. Subsequently, the same models were fitted using only the ASVs, which had a variable importance for classification greater than zero in the best random forest model (best RF). Finally, a model was fitted using only the taxa with

the highest variable importance in the best RF model (top 99th percentile). This procedure should remove noisy ASVs and retain only the most informative taxa characterizing the microbial communities of healthy and diseased oysters.

3 Results

For the bacterial 16srRNA dataset, a total of 7,023,546 reads were initially assigned to 17,982 taxa after passing through the quality filters of the dada2 pipeline for both host species. Among these reads, 4,362,842 were assigned to *O. edulis* samples. After filtering out singletons and taxa with a total relative abundance of less than 12, we retained 4,348,967 reads (99.68%) belonging to 4,155 taxa across 189 samples. Subsequently, the dataset was rarefied to 10,000 reads per sample, resulting in a final 16s rRNA dataset for *O. edulis* with 4,112 bacterial taxa observed across 165 samples. The remaining 2,660,704 reads were assigned to the *M. gigas* samples. Taxa were filtered by removing those with a relative abundance below 10, which resulted in retaining 99.67% of the reads distributed across 3,490 ASVs in 95 samples. Rarefaction was applied to standardize the data to 10,000 reads per sample, resulting in a final 16s rRNA dataset for *M. gigas* consisting of 3,428 bacterial taxa observed across 91 samples.

The eukaryotic microbiome dataset comprised a total of 6,624,391 reads assigned to 8,813 taxa after the initial quality filtering process. Among these reads, 3,891,196 came from *O. edulis* samples. After applying relative abundance-based taxon filtering with a cut-off of less than 10, 99.86% of the reads were retained, resulting in 2,937 taxa observed across 158

samples. The dataset was further rarefied to 10,000 reads per sample, resulting to 2,853 taxa in 150 samples.

In the case of the eukaryotic microbiome of *M*. gigas, 99.85% of the 2,733,195 reads were retained after relative abundance filtering, using a cut-off value of 14. This filtering step resulted in a total of 1,295 taxa observed across 92 samples. Rarefaction analysis removed only one additional ASV, leaving a final dataset of 1,294 taxa observed across 92 samples.

3.1 Diversity within body compartments and infection states

Taxonomic composition varied strongly between body compartments in *O. edulis* (Fig. 1). Consequently, the ASV-level diversity of the prokaryotic microbiome, measured in terms of the number of different ASVs and Shannon index, exhibited significant variation as well. In contrast, the variation explained by infection state was comparatively lower (Table 2). The overall absence of an infection effect in *O. edulis* can be attributed to a significant interaction between tissue type and infection. Specifically, there were no effects on diversity in the gill tissue, an increase of diversity in the digestive gland tissue, and a decrease in diversity in the fluid body compartments (hemolymph and pallial fluid) observed for *Marteilia*-infected *O. edulis* (Fig. 1A). In the case of *Bonamia* infection, no significant effects on prokariotyc diversity estimates were detected (Fig. 1A).

Regarding *M. gigas*, significant differences in the number of taxa were observed between body compartments, but these differences were not reflected in the Shannon diversity index. A significant interaction between tissue type and infection was found (Table 2). This difference was driven by a decrease in diversity in the digestive gland, while increased diversity was observed in the hemolymph and pallial fluid. This pattern was opposite to the observed effects of *Marteilia* infection in *O. edulis* (Fig. 1 A,C).

Table 2: Wald χ^2 analyses of deviance based on linear mixed models of alpha diversity measures (# of ASVs, Shannon index) for pro- and eukaryotic microbiomes in different body compartments of infected and uninfected oysters. The sample sizes for each group can be found in Table 1.

		Effect	O. edulis χ^2	df	p	M. gigas χ^2	df	p
Prokaryote	# of ASVs	Tissue (T)	**43.849**	**3**	**<0.001**	**15.688**	**3**	**0.001**
		Infection (I)	2.052	2	0.359	0.139	1	0.709
		T * I	**17.989**	**6**	**0.006**	7.414	3	0.059
	Shannon	Tissue (T)	**34.124**	**3**	**<0.001**	4.354	3	0.226
		Infection (I)	5.950	2	0.051	1.636	1	0.201
		T * I	**23.278**	**6**	**<0.001**	**9.000**	**3**	**0.029**
Eukaryote	# of ASVs	Tissue (T)	**52.158**	**3**	**<0.001**	5.707	3	0.127
		Infection (I)	0.844	2	0.656	1.967	1	0.161
		T * I	4.816	6	0.568	3.933	3	0.269
	Shannon	Tissue (T)	7.578	3	0.056	5.304	3	0.151
		Infection (I)	**8.603**	**2**	**0.014**	**4.115**	**1**	**0.043**
		T * I	**15.203**	**6**	**0.019**	4.368	3	0.224

We observed qualitative differences between the microbiome compartments with regard to infection state. In *O. edulis*, the prokaryotic communities showed increased diversity in the digestive gland and reduced diversity in the fluid body compartments when infected by *Marteilia*. However, there was no significant effect on diversity when infected by *Bonamia*. On the other hand, the eukaryotic community exhibited reduced diversity in the solid body compartments when infected by *Marteilia* (digestive gland) or *Bonamia* (digestive gland and gills), while no effect on diversity was observed in the fluid body compartments (hemolymph and pallial fluid, Fig. 1B). In *M. gigas*, the diversity of eukaryotic communities was more consistent across body compartments, with a comparatively weak effect of OsHV-1 infection associated to reduced Shannon diversity in all body compartments. However, this effect was

only significant for the digestive gland and was only partially reflected in the number of taxa (Table 2, Fig. 1D). Overall, our findings suggest that infections by eukaryotic parasites in *O. edulis* had stronger and more tissue-specific effects compared to viral infection in *M. gigas*. Changes in diversity were dependent on the specific combination of tissue type and parasite, resulting in increased diversity in the digestive gland but reduced diversity in fluid body compartments when infected with *Marteilia,* and the opposite pattern was observed for OsHV-1 infections in *M. gigas*. *Bonamia* infection, on the other hand, primarily affected eukaryotic diversity in solid body compartments. These results demonstrate that the effects of different infections on to microbiome are compartment-specific and dependent on the combination of pathogen species and the affected tissue, rather than showing a general unidirectional change in diversity (e.g. reduced diversity).
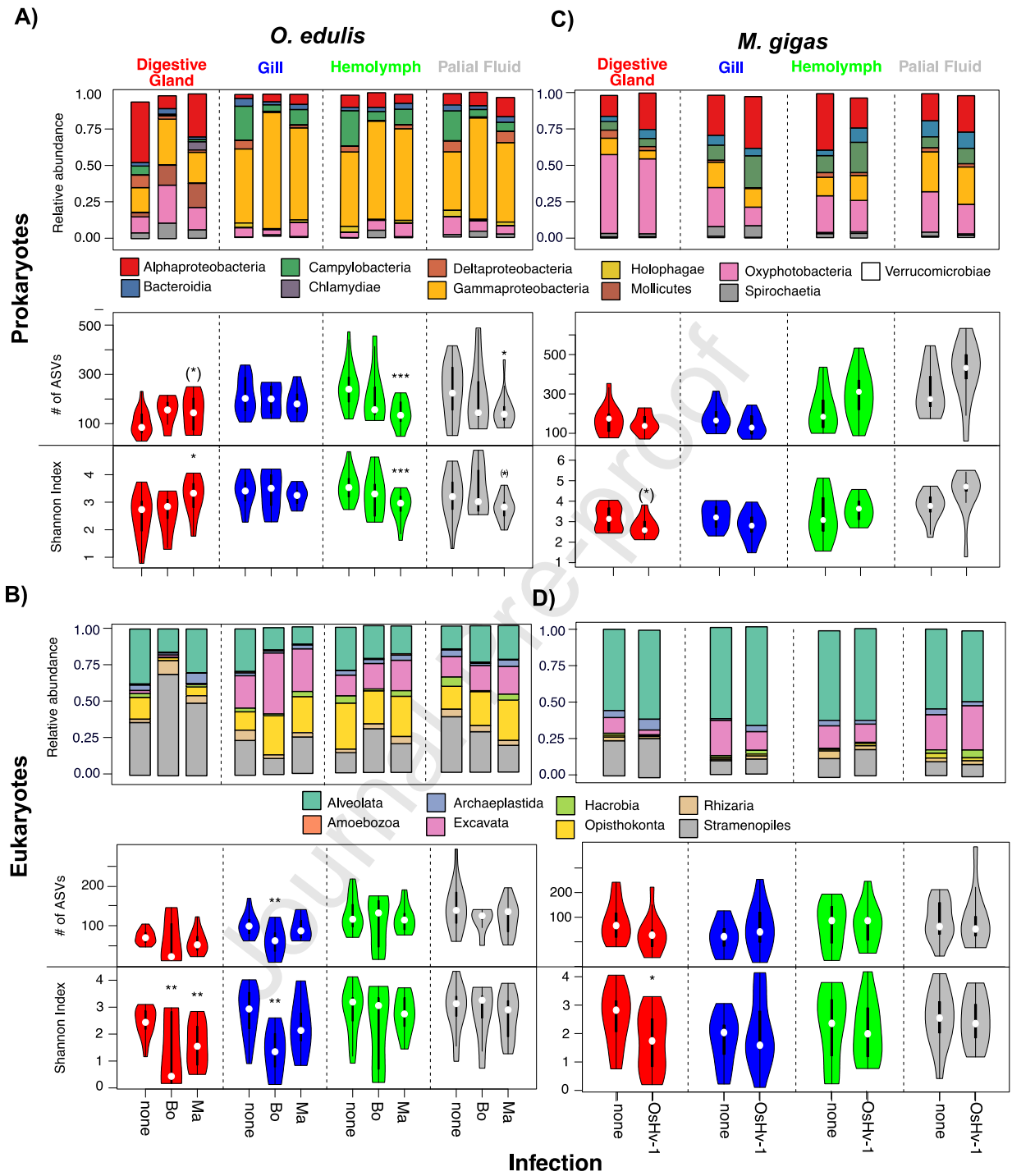
Figure 1: Class-level taxonomic composition and ASV-level alpha diversity, expressed as the number of ASVs and Shannon index, of microbiota in different body compartments of infected and uninfected oysters. Prokaryotic microbiota are shown in the upper panels (A, and C). Supergroup-level taxonomic composition and alpha diversity

of eukaryotic microbiota are shown in the lower panels (B and D). The left panels (A and B) show the tissue-specific microbiomes of *O. edulis* infected with *Bonamia ostreae* (Bo) and *Marteilia refringens* (Ma), and the right panels show the microbiomes of *M. gigas* infected with OsHV-1. Taxonomic composition gives the relative abundance as the proportion of all reads after adding up all reads within each combination of species, body compartment and infection state. Only taxa contributing >5% are shown. Violins display the density distribution of the value range, boxes represent the 25th to 75th, and whiskers represent the 5th to 95th quantile, while white dots indicate the median. Asterisks above violins of infected groups indicate significant differences to uninfected oysters within the respective tissue, obtained from linear models calculated for each tissue (***: $p < 0.001$, **: $p < 0.01$, *: $p < 0.05$, (*): $p < 0.1$).

3.2 Differentiation between body compartments and infection states

The composition of microbial communities exhibited significant differences between body

compartments in all comparisons when considering the entire community (Fig. 1, all ASVs in Table 3).

The variation in community composition attributed to body compartment ranged from 7.4% to 20.0%.

The differences between infection states, on the other hand, accounted for a smaller proportion of

variation, ranging from a non-significant 0.9% for eukaryotic communities in *M. gigas* to 4.9% for

prokaryotic communities in *O. edulis*. These differences were also noticeable on the class- and

supergroup level taxonomic composition (Fig. 1). Notably, eukaryotic communities consistently

explained a lower proportion of variation compared to prokaryotes. The specific combination of

infection state and tissue did not significantly contribute to the variation observed in the underlying

distance matrices (Table 3), indicating that the effect of infection was comparable across different body

compartments. However, when the number of ASVs was reduced to only include taxa identified as

important in random forest classification (with variable importance >0), the proportion of variation

explained by infection state increased. This effect was enhanced when only the most important taxa

were retained (Table 3). This reduction in the dataset to taxa identified by the best fitting random forest

model resulted in the removal of 87% to 96% of taxa, leading to improved differentiation between

infection states in both species (improvement ranging from 0.1% to 1.0%). The reduction of ASV

variables also slightly increased differentiation between body compartments, particularly for

prokaryotic communities (0.7% and 0.2%) and to a greater extent for eukaryotes (1.5% and 1%, see

Table 3). These trends were further amplified when only taxa with the highest variable importance

(99% quantile) were retained in the dataset. This drastic reduction in the number of ASVs by >99% in all

cases confirmed that "noisy" taxa, which had low variable importance, did not contribute significantly

to community differentiation between infection states and body compartments (Table 3). Specifically,

the community variation explained by infection increased by 3.5% and 3.1% for prokaryotic

communities in *O. edulis* and *M. gigas*, respectively. In contrast, there was only a 1% and 1.2% increase for eukaryotes, with no significant effect of infection state or tissue observed in *M. gigas* (Table 3). These results demonstrate the effective reduction of noise from the data by efficiently maximizing meaningful differences with a comparatively small subset of taxa variables through our classification strategy. Furthermore, the improved differentiation between infection states was more pronounced in prokaryotic communities compared to eukaryotic communities, where variable reduction primarily enhanced differentiation between body compartments.

Table 3: Permanova results of fitting infection state (I) and tissue (T) and their interaction (I*T) to the full dataset (all ASVs), the best random forest model, and the most important taxa of that RF model for prokaryotic and eukaryotic microbiomes of *O. edulis* and *M. gigas*.

				All ASVs			Best Random Forest (best RF)			Most important taxa from best RF		
		Factor	Df	F	P	R²	F	P	R²	F	P	R²
O. edulis	Prokaryote	Infection (I)	2	4.54	<0.001	0.049	5.241	<0.001	0.055	8.31	<0.001	0.084
		Tissue (T)	3	6.176	<0.001	0.099	6.687	<0.001	0.106	7.593	<0.001	0.115
		I * T	6	0.944	0.629	0.03	0.905	0.657	0.029	0.879	0.652	0.027
				4112 taxa in 165 samples			*421 taxa in 165 samples*			*17 taxa in 165 samples*		
	Eukaryote	Infection (I)	2	3.34	<0.001	0.041	3.46	<0.001	0.042	4.323	<0.001	0.051
		Tissue (T)	3	4.163	<0.001	0.078	5.062	<0.001	0.093	7.981	<0.001	0.141
		I * T	6	1.201	0.067	0.045	1.249	0.056	0.046	1.115	0.307	0.039
				2758 taxa in 146 samples			*332 taxa in 165 samples*			*8 taxa in 143 samples*		
M. gigas	Prokaryote	Infection (I)	1	2.087	0.018	0.019	3.227	0.004	0.029	5.470	<0.001	0.050
		Tissue (T)	3	7.327	<0.001	0.200	7.542	<0.001	0.202	6.054	<0.001	0.165
		I * T	3	0.902	0.624	0.025	1.031	0.394	0.027	1.173	0.261	0.032
				6369 taxa in 91samples			*287 taxa in 91 samples*			*11 taxa in 91 samples*		
	Eukaryote	Infection (I)	1	0.845	0.515	0.009	0.915	0.462	0.010	1.894	0.111	0.021
		Tissue (T)	3	2.312	<0.001	0.074	2.652	0.003	0.084	0.933	0.481	0.031
		I * T	3	0.709	0.858	0.023	0.702	0.834	0.022	0.513	0.890	0.017
				1294 taxa in 92 samples			*174 taxa in 92 samples*			*4 taxa in 92 samples*		

3.3 Infection state classification

The classification of known infection states on the relative abundance of microbial taxa qualitatively confirmed the results of the PERMANOVA analysis. In all body compartments, the infection state could be predicted more accurately using prokaryotic compared to eukaryotic microbiota using random forest-based machine learning. For both host species, the accuracy and area under the curve (ROC) obtained from training sets indicated high prediction accuracy. This high accuracy also translated into relatively low overall classification errors of 24.4% and 28.4% for *O. edulis* and *M. gigas*, respectively (Table 4). However, the classification errors were not symmetric, as the uninfected individuals could be predicted with high accuracy for both oyster species (9.5% and 17.6% error rates). Classification errors for infected individuals, whether by parasite or viral infection, were higher. Despite high classification errors ranging from 35% to 50%, the majority of infected individuals were correctly assigned to their true infection state (Table 4).

The eukaryotic microbiomes displayed significantly lower classification precision, resulting in overall error rates of 45.4% and 41.2%. In *O. edulis*, correct classification was higher in uninfected individuals (27.5% error rate), but poor for infected individuals (error rates 54.1% - 75%, Table 4). In *M. gigas* however, classification as uninfected was incorrect in 45.7% of the cases, while only 36.3% of OsHV-1 infected individuals was wrongly classified as uninfected (Table 4). These results further support our findings on alpha- and beta-diversity, indicating that differences in the prokaryotic microbiota are more strongly associated with infection than differences in the eukaryotic microbiota.

Table 4: Random forest classification of infection states based on prokaryotic and eukaryotic microbiota. Classification statistics are given for the training and test set (accuracy: correct assignments in the test data set, ROC: area under the curve, mtry: number of parameters used) and the final model fitted to the complete data set. Shaded cells in the confusion matrix show correct assignments and bold numbers show the most commonly assigned class for each original group. Error gives the proportion of wrongly assigned individuals for each group and the overall error rate in bold.

O. edulis — prokaryote

accuracy	ROC	mtry	Confusion matrix	none	*Bonamia*	*Marteilia*	Error	
0.833	0.933	594	none	**57**	0	6	0.095	
			Bonamia	4	**10**	6	0.5	**0.244**
			Marteilia	14	0	**26**	0.35	

O. edulis — eukaryote

accuracy	ROC	mtry	Confusion matrix	none	*Bonamia*	*Marteilia*	Error	
0.421	0.629	802	none	**37**	2	12	0.275	
			Bonamia	9	5	6	0.75	**0.454**
			Marteilia	**19**	1	17	0.541	

M. gigas — prokaryote

accuracy	ROC	mtry	Confusion matrix	none	OsHV-1	Error	
0.708	0.750	1090	none	**28**	6	0.176	
			OsHV-1	13	**20**	0.394	**0.284**

M. gigas — eukaryote

accuracy	ROC	mtry	Confusion matrix	none	OsHV-1	Error	
0.542	0.503	277	none	**19**	16	0.457	
			OsHV-1	12	**21**	0.363	**0.412**

3.4 Indicator taxa contributing to differentiation

To identify indicator species that reflect the different infection states, their relative abundance compared to uninfected oysters needs to be determined. For the prokaryotic indicators of *O. edulis*, we were able to identify tissue-specific significant differences in relative abundance differences for 14 out of the 17 taxa of high importance (Fig. 2B). In *Marteilia* infections, seven taxa showed increased relative abundance in at least one tissue (ASV75: *Mycoplasma*; ASV3, ASV37: *Vibrio*; ASV151, ASV374: *Photobacterium*, ASV1886: undetermined Alphaproteobacteria; ASV549: unknown taxonomic affiliation) and one showed decreased relative abundance in the hemolymph (ASV1231: *Motilliproteus*). In *Bonamia* infections, also seven taxa displayed higher relative abundance (ASV835: *Acanthopleuribacter*; ASV904, ASV1231: *Motilliproteus*, ASV361: *Amphritrea*; ASV1703: SAR324; ASV15, ASV145: *Arcobacter*). We also found two ASVs with significantly reduced relative abundance (ASV37: *Vibrio*; ASV151: *Photobacterium*, see Fig. 2). Among the three significant taxa that were shared between infections, two showed opposing patterns in the same tissue (ASV1231: *Motilliproteus* in Hemolymph and ASV37: *Vibrio* in pallial fluid). The differences in significance patterns between body compartments were most pronounced between the digestive gland and the other body compartments. We found the most significant differences between infected and uninfected animals in the pallial fluid (12), while we found nine significant differences in gill tissue and only seven in hemolymph and digestive gland. This pattern was also partly reflected in the ordination plot, where the largest overlap between infection stages was observed in the digestive gland, while stronger group separation was observed in gills and hemolymph (especially between *Bonamia* and *Marteilia* infections, Fig. 2A).
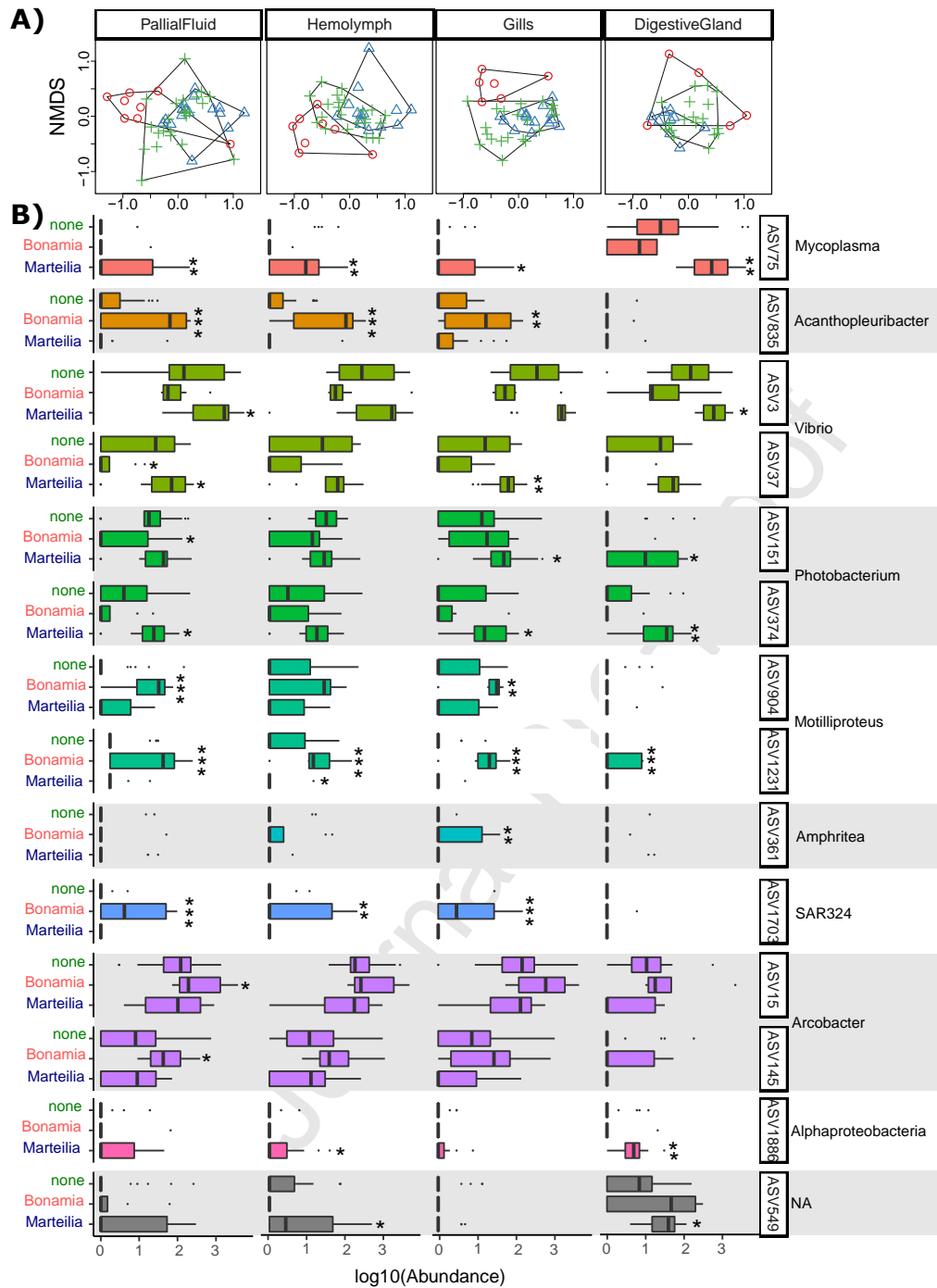
Figure 2: Prokaryote taxa contributing to differentiation between infection states in *O. edulis*. A) Tissue-specific

NMDS plots display the communities of the 17 most influential taxa in distinguishing between infection states (red

circles: *Bonamia*, blue triangles: *Marteilia*, green crosses: uninfected). B) Boxplots present the log-transformed

relative abundance of the 14 taxa that showed significant differences between one infection and uninfected

oysters in at least one of the investigated body compartments. The median is depicted as a vertical line, the box represents the 50% quantile, and the whiskers display the 95% quantile. Only taxa showing a significant difference in GLM analyses between uninfected oysters and one of the two infections are shown (indicated by asterisks:*** for p < 0.001, ** for p< 0.01, * for p<0.05).

The differentiation of eukaryotic communities in *O. edulis* exhibited distinct behavior compared to prokaryotes. We observed the most significant differences in the digestive gland (7), whereas only two significant differences were found in each of the other body compartments. This was also reflected in the greater overlap in NMDS ordinations for these body compartments (Fig. 3). Overall, we identified tissue-specific relative abundance differences for all eight taxa. In *Marteilia* infections, three ASVs showed higher relative abundance: asv1095 (*Euduboscquella* sp.) in the digestive gland and pallial fluid, asv0451 (*Hymeniacidon kitchingi*) in the gills, and asv0245 (*Thalassosira delicatula*) in the digestive gland. Additionally, two ASVs were associated with lower relative abundance: asv0282 (unknown gregarine) in the digestive gland and asv0022 (unknown Alveolata) in the hemolymph.

In *Bonamia* infections, we observed significantly higher relative abundance for two taxa: asv0778 (unknown bicosoecid) in the digestive gland and hemolymph, and asv0022 (unknown Alveolata) in the digestive gland. On the other hand, three taxa showed reduced relative abundance: asv0003 (unknown kinetoplastid) in the pallial fluid and gills, asv0018 (unknown Thalassiosirales) in the digestive gland and hemolymph, and asv0282 (unknown gregarine) in the digestive gland. There was only minimal overlap between the taxa associated with *Bonamia* infections and those associated with *Marteilia* infections. Specifically, the unknown gregarine asv0282 showed reduced relative abundance in the digestive gland of both infections, while the unknown Alveolate asv0022 exhibited opposite trends but in different body compartments. This suggests that eukaryote diversity is primarily affected in the digestive gland, and different taxa can be positively or negatively associated with both infections.
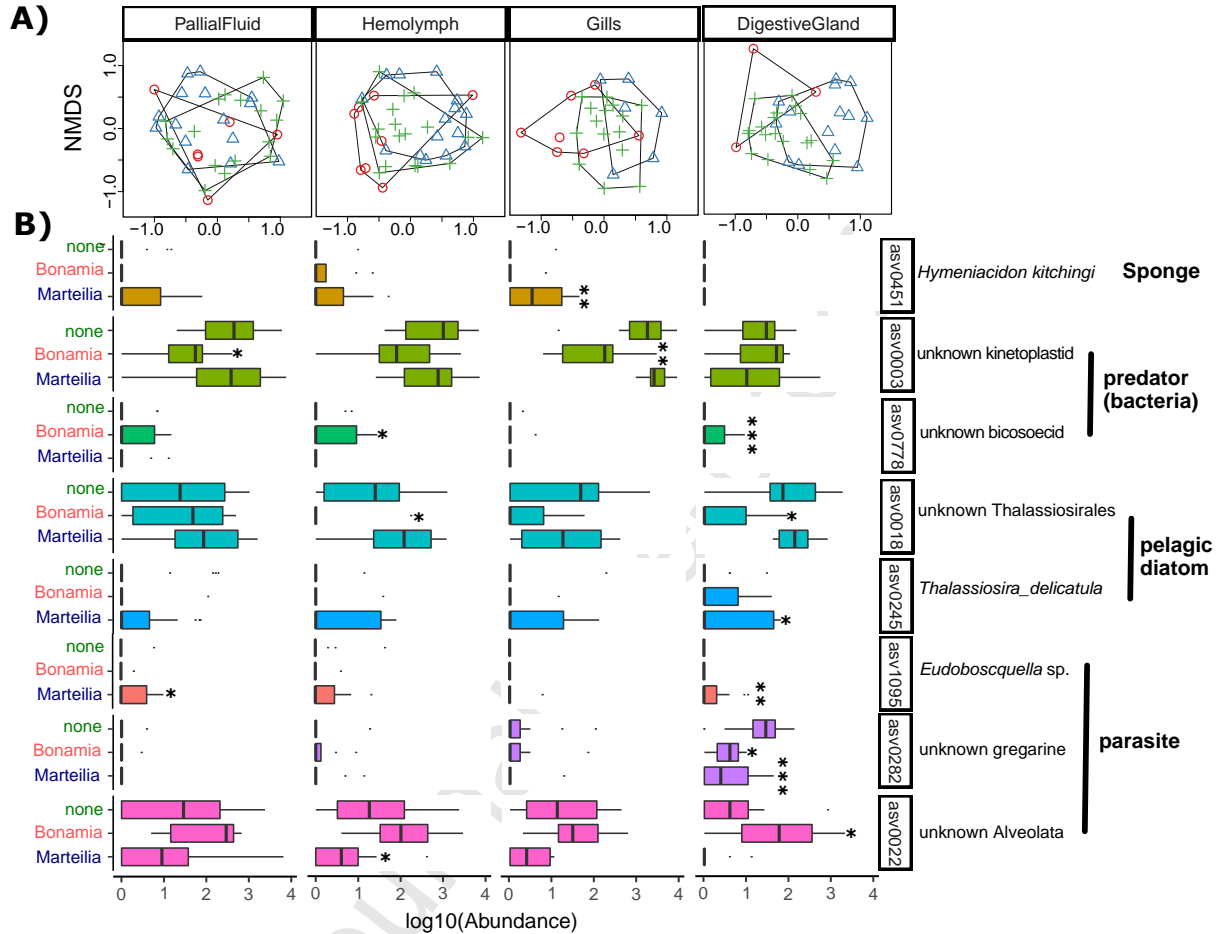
Figure 3: Eukaryote taxa contributing to differentiation between infection states in *O. edulis*. A) Tissue-specific NMDS plots representing the communities of the 8 taxa that have the most significant contribution to differentiating between infection states (red circles: *Bonamia*, blue triangles: *Marteilia*, green crosses: uninfected). B) Boxplots present the log-transformed relative abundance of individual taxa that showed significant differences between the three infection states in at least one of the investigated body compartments. The median is represented by a vertical line, the box represents the 50% quantile, and the whiskers indicate the 75% quantile. Significant differences between uninfected oysters and either one of the two infections are marked by asterisks (*** for p < 0.001, ** for p< 0.01, * for p<0.05).

The differentiation between infection states in *M. gigas* was weaker compared to *O. edulis* (Table 3). This was evident in the less pronounced distribution of variable importance of taxa identified by random forest classification. The best random forest model for *M. gigas* included fewer prokaryotic taxa compared to *O. edulis* (287 vs. 421). Additionally, the 99th percentile of high importance taxa contained only 11 taxa in *M. gigas*, whereas 17 taxa were retained for *O. edulis* (Table 3). Out of these 11 taxa, we found tissue-specific differences between infected and uninfected individuals in only 6 taxa. Most differences were found in the tissue body compartments (gills and the digestive gland), with four significant differences in each. The liquid body compartments showed fewer differences in the relative abundance of high importance taxa (hemolymph: 1 difference and pallial fluid: 2). For instance, higher relative abundances of two chloroplasts (ASV102 and ASV1138) were observed in the digestive gland and gill tissue of uninfected oysters (Fig. 4). Similarly, ASV4 (*Mycoplasma*) showed a higher relative abundance in the gills and pallial fluid of uninfected *M. gigas*. On the other hand, two *Helicobacteriaceae* (ASV11 and ASV276) were more abundant in all body compartments, and an unidentified Gammaprotebacterium (ASV938) was more abundant in the digestive gland of infected individuals (Fig. 4). The differentiation between the eukaryotic communities of infected and uninfected *M. gigas* was not significant (Table 3). Consequently, we could not identify any significant differences in the four taxa of high importance identified by the random forest classification.
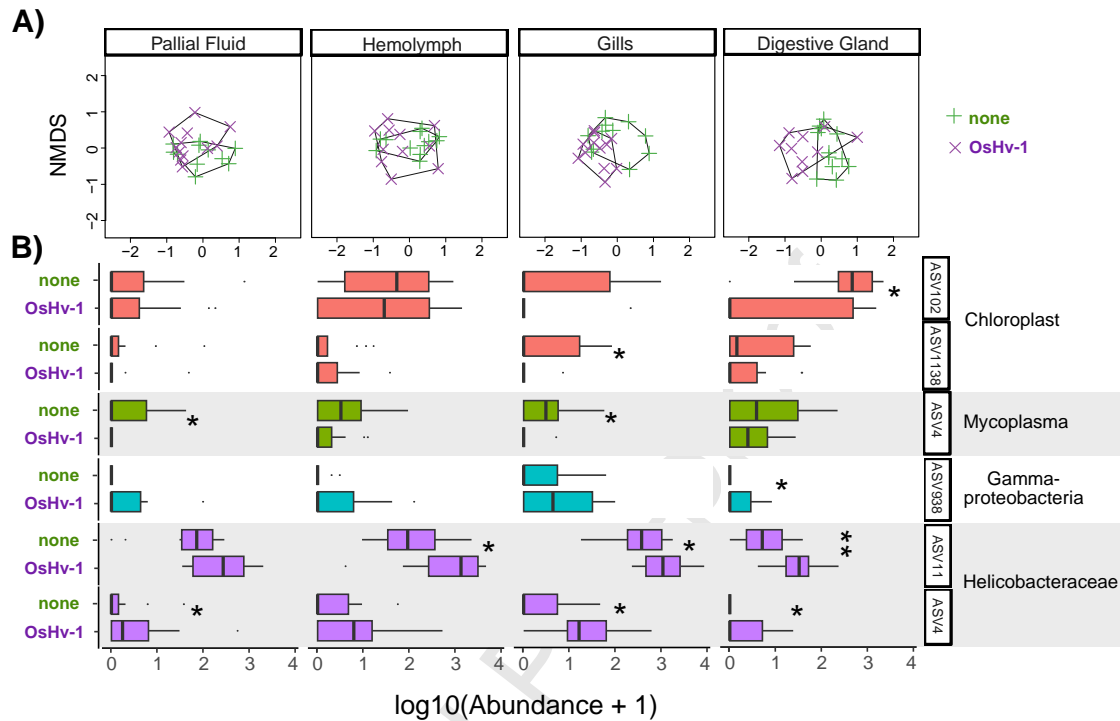
Figure 4: Prokaryote taxa contributing to the differentiation between infection states in *M. gigas*. A) Tissue-specific NMDS plots representing the communities of the 11 taxa contributing most to the differentiation between infection states (purple x-crosses: OsHV-1, green crosses: uninfected). B) The log-transformed relative abundance of individual taxa that showed significant differences between the two infection states in at least one of the investigated body compartments is displayed in boxplots. The vertical line represents the median, the box represents the 50% quantile, and the whiskers represent the 75% quantile. Only taxa with a significant difference between uninfected oysters and oysters with OsHv-1 infection are shown (marked by asterisk: ** for p< 0.01, * for p<0.05).

4 Discussion

The influence of host-associated microbiota on disease outcome in marine bivalves has been the subject of numerous studies (Paillard et al., 2022). However, our understanding of the intricacies of this relationship remains incomplete, and fundamental principles are still unknown. One of the unanswered questions pertains to how different classes of microbes interact with different diseases. Most studies have focused on single diseases and bacterial microbiota, despite the fact that marine bivalves harbor a diverse array of microbes, including viruses, bacteria and protists (Dupont et al., 2020). Protists in particular have been underexplored in comparison to bacterial microbiota, despite the potential for interactions between protist microbiota and protist pathogens (Clerissi et al., 2020b). By characterizing the bacterial and protist microbiomes in three prevalent diseases affecting two oyster species, we were able to demonstrate that bacterial microbiota were more effective in discriminating infected from uninfected hosts, even when the infectious agent was a protist itself. The superior discriminative power of prokaryotic microbiota was consistently observed across host-disease combinations and all analytical approaches, indicating that the structural and compositional diversity of bacterial communities are likely to capture more relevant aspects of host-associated microbes than protist communities in the context of disease in these two oyster species. To identify indicator taxa that played a significant role in differentiating between the infected and uninfected individuals, we employed random forest machine learning. This approach represents a significant advancement in the discriminatory capabilities of microbiome studies. The relatively small number of resulting indicator taxa helped mitigate statistical overfitting (Broadhurst and Kell, 2006) and maximized the differences between bacterial communities of infected and healthy individuals. Consequently, these indicator taxa may hold valuable potential for identifying early stages of infection risks or developing probiotic treatments (Kesarcodi-Watson et al., 2012). The fact that prokaryotic microbiota provide more information than protist communities about infection states was consistent in different species and diseases coming from different environments. This makes our inference of associations between a

relatively small number of prokaryotic microbiota and disease quite robust. However, the identity of these indicator taxa will inevitably harbor an environmental component. Further experimental verification in a wider geographic context are needed to separate general patterns from population specific environmental effects.

4.1 Structural and compositional differences between infection states

The targeted diseases encompassed a diverse range of pathogens, including a virus and two protists. These pathogens exhibit distinct tropisms in different host tissues. For instance, *Marteilia refringens* primarily infects the digestive epithelium of flat oysters (Grizel, 1979), while *Bonamia ostreae* predominantly infects within hemocytes found in various tissues, particularly the gills (Comps et al., 1980; Pichot et al., 1979). These differences in tropism were only partially reflected in structural aspects of the microbiota, and the different classes of microbes showed contrasting reactions. Regarding individual alpha-diversity in bacterial communities of *O. edulis*, distinct differences were observed only in individuals infected with *M. refringens*. In this case, there was an increase in diversity in the site of infection (digestive gland), but a reduction in hemolymph and pallial fluid (Fig. 1A). Similarly, studies in other oyster species infected by protists also reported reduced diversities across a variety of tissues. For example, the digestive glands of *Saccostrea glomerata* infected by *Marteilia sydneyi* were dominated by a single Rickettsiale-like phylotype, whereas uninfected individuals contained over 20 phylotypes in 16s rRNA clone libraries (Green and Barnes, 2010). When utilizing 16s rRNA metabarcoding on the same species, bacterial alpha-diversity was reduced in the adductor muscle (Nguyen et al., 2021). However, these studies did not investigate other tissues. In the case of *C. virginica* infected by *P. marinus*, comparisons across multiple tissues and body fluids only revealed reduced diversity in inner shell samples (Pimentel et al., 2021). This suggests that specific patterns of diversity change in a pathogen and tissue dependent manner. On top of that environmental variation will play a role. Environmental variation does not necessarily exceed variation between species (Paillard et al.,

2022), but general patterns may be challenging to identify, even within species infected by the same parasite/pathogen.

Similarly, the effects of viral infection in *M. gigas* do not always show consistent patterns. Some studies have associated susceptibility or infection with reduced diversity (Clerissi et al., 2020a; King et al., 2019a), which aligns with ours findings for the digestive gland and gill tissue (Fig. 1C). On the other hand, other studies have identified higher alpha diversity across infection stages (de Lorgeril et al., 2018), reflecting our results for the pallial fluid. While significant shifts in diversity, as seen in *M. refringens*-infected *O. edulis*, could indicate dysbiosis, the inconclusive patterns observed across studies suggest that variation in alpha-diversity may not be a consistent and reliable indicator for different diseases. Nevertheless, we observed stronger shifts between infected and uninfected individuals for prokaryotic diversity.

On the other hand, the tropism of protist infection in *O. edulis* was better reflected in eukaryotic communities than in bacterial communities, as both infected tissues (gills for *B. ostreae*, digestive gland for *M. refringens*) showed a significant reduction in diversity. However, it is important to note that these reductions could at least partly influenced by our removal of *Bonamia* and *Marteilia* sequences from the datasets before analysis. With no significant differences observed in *M. gigas*, this would leave only the reduced protist diversity in the digestive glands of *Bonamia*-infected oysters as an example of alpha-diversity modification by infection. Direct competition between protists is more conceivable than competition between protists and bacteria. Indeed, we observed reduced abundances of other parasitic apicomplexans in infected individuals, which could be interpreted as a sign of such competition leading to reduced community diversity. However, at the community level, these potential competitive interactions did not result in unimodal effects on alpha-diversity, and stronger effects were still observable for prokaryotic communities.

The higher information content of bacterial microbiota was also evident in the variation between individuals, both visually in the ordinations (Fig. 2A vs. Fig. 3A) and in the PERMANOVA analyses (Table 3). Although we observed significant differentiation between infections states in eukaryotic microbiota in *O. edulis,* the amount of explained variation was considerably lower than that of the prokaryotic communities and could only be marginally improved by removing noisy taxa (Table 3). Overall, the community shifts associated with OsHV-1 infection in *M. gigas* were weaker compared to the shifts associated with protist infections in *O. edulis,* and less than half of the compositional variation associated with protist infections in *O. edulis* could be accounted for (Table 3). This discrepancy could be partly explained by the biology of the infectious agents. *B. ostreae* and *M. refringens* are considered chronic infections that persist over relatively long periods, allowing more time for the microbial communities to respond and shift in response to infection. In contrast, OsHV-1 development can occur rapidly, leaving less time for microbial community changes to occur. Other studies have shown strong differentiation between uninfected and infected oysters in the late stages of OsHV-1 infection (de Lorgeril et al., 2018; King et al., 2019a). We attempted to address this by including samples from OsHV-1 infected oysters collected before and during disease outbreak, but it is possible that we still missed relevant time frames to capture microbial community shifts. The lack of differentiation observed here could be partially attributed to low virus titers in infected *M. gigas* (maximum of 363 virus copies/ng of DNA extract), reducing the overall effect on infected oysters. The bacterial dysbiosis observed in previous studies following immune suppression by OsHV-1 infection shortly before oyster death (de Lorgeril et al., 2018) was likely not observed here since we only sampled non-moribund oysters, even during the disease outbreak. Nevertheless, the presence of viruses either left some traces in the bacterial communities, but not in the protist communities.

The clearest distinction between prokaryotic and eukaryotic community responses was obtained through the random forest classification. In this analysis, the prediction accuracy was 1.97 times higher

for prokaryote microbiota in *O. edulis* and 1.57 times higher for *M. gigas* (Table 4). The classification of infection states in both oyster species also reflected the more pronounced community shifts observed in *O. edulis* (Table 4). This suggests that random forest machine learning may be the most sensitive method used in this study to characterize infection states and identify taxa that drove community shifts associated with infection. Taken together, the combination of multiple methodological approaches in multiple host species affected by different diseases provided compelling evidence that disease states can be better distinguished by prokaryotic rather than eukaryotic microbiota. Furthermore, the random forest classification was able to identify a relatively small number of indicator taxa (less than 17) that maximize differentiation between infection states. The exact number and identity of taxa maximizing differentiation between infection states is likely to be specific for the samples used here. Nevertheless, it can generally be expected that random forest classification or other machine learning algorithms will be able to efficiently separate informative from noisy taxa and thereby reduce the complexity of target microbial communities in the context of disease.

4.2 Indicator taxa characterizing infection states

Due to the low discriminative power of eukaryote communities between infection states we did not find any eukaryotic indicator taxa in *M. gigas* and only a few in *O. edulis* (Table 3,4; Fig. 3). The differences observed were concentrated in the digestive gland (7 out of 14, Fig. 3), which is likely one of the preferred habitats for protists in bivalves (Słodkowicz-Kowalska et al., 2015). Out of the eight indicator taxa identified, only diatoms affiliated to the taxon *Thalassiosira* have been previously described as part of the eukaryotic microbiota in *M. gigas* (Clerissi et al., 2020b). However, with only one other study describing protist microbiota in oyster species, the available data for comparisons is very limited. The indicator taxa asv0245 and asv0018, both classified as pelagic diatoms and asv0451 (*Hymeniacidon kitchingi*, sponge),

can be considered as food items or environmental RNA (eRNA) and may not be part of the host-associated microbiota but rather reflect differences in filtration activity. On the other hand, the biggest group of indicator protists were classified as Alveolata, which are all potential unicellular parasites (asv1095, asv0282, asv0022, Fig. 3). These taxa have not been described as parasites of molluscs. Nevertheless, the dependence of infection patterns of potential parasites on the infection state of our focal parasites might indicate that infection with one parasite might over-proportionally influence the infections patterns with other parasites. The relative abundance patterns of these protists across infection states and body compartments were however quite variable. For example, the reference sequence of asv0282 (unknown gregarine) was closely related to a gregarine symbiont described from tunicates (Rueckert et al., 2015), and showed a decreased relative abundance in the digestive gland in both *Marteilia* and *Bonamia* infections. In contrast, asv0022 (unknown Alveolata) increased in the digestive gland in *Bonamia* infection but decreased in the hemolymph in *Marteilia* infections. Asv1095 (*Eudoboscquella sp.*) described as a parasite of tintinnids, increased in the digestive gland of *Marteilia*-infected *O. edulis*. Also, other functional groups like predators of bacteria did not show uniform patterns. The asv0003 (an unknown kinetoplastid) decreased in the gills and pallial fluid, whereas asv0778 (unknown bicosoecid) increased in the digestive gland and hemolymph with *Bonamia* infections. These variable patterns across body compartments and infections might further explain the lower discriminatory power of eukaryotic microbiota.

In contrast, bacterial indicator taxa displayed a more even distribution across body compartments, and most differences were found in pallial fluid (12 out of 35, Fig. 2). A closer

examination revealed that several taxa also reflected the tropism of infection, with tissue-specific relative abundance patterns matching the infection sites of different parasites. For example, asv75 (*Mycoplasma*) was found in higher numbers in the digestive gland of uninfected oysters (Fig. 2B). However, when an oyster was infected with *M. refringens*, we observed a significant increase in the abundance of this ASV not only in the digestive gland but also the other investigated body compartments. The strong increase of ASV75 in its original digestive gland tissue might have led to spill-over to other body compartments (Fig. 2B). This spread through different organs associated with parasite infection may explain the absence of stronger tissue-specific effects of infection (tissue x infection interaction in Table 2). *Mycoplasma* spp. is known to be an abundant symbiont in the gut microbiota of bivalves (Aceveses et al., 2018; Lokmer, Ana et al., 2016; Pierce and Ward, 2019), and its reduced metabolism, as well as its dependence on host-derived nutrients, suggests that it might be able evolve a parasitic lifestyle (Pimentel et al., 2021). Similar patterns of organism-wide spread of *Mycoplasma* ASVs in relation to parasite infection have been observed in *O. edulis* exposed to *Phaeobacter inhibens* and *M. gigas* infected by OsHV-1 (Delisle et al., 2022; Dittmann et al., 2019). Other studies have reported reduced relative abundances of *Mycoplasma* in the adductor muscle of *S. glomerata* in response to infection by *Marteilia sydneyi* (Nguyen et al., 2021) and in several tissues of *Crassostrea virginica* infected with *Perkinsus marinus* (Pimentel et al., 2021). These opposing results stem from different host species sampled at different sites and environments. This variability suggests that the role of *Mycoplasma* in the oyster microbiome, as well as its response to parasite infection, may be species and/or environment specific. Therefore, it emphasizes the need for a specific

evaluation of microbial roles as beneficial/probiotic strains or markers for infection and disease in different host-parasite combinations (Offret et al., 2020).

In addition to *Mycoplasma*, we also observed similar but less pronounced patterns of increased relative abundances in oysters infected with *M. refringens* originating from the digestive gland for other ASVs including ASV3, ASV37 (*Vibrio*), ASV151, ASV374 (*Photobacterium*). These taxa, along with *Mycoplasma*, are potential agents of disease themselves (Le Roux et al., 2016; Pira et al., 2022) or are commonly found in bacterial communities of stressed oysters (Wegner et al., 2013) undergoing dysbiosis (de Lorgeril et al., 2018; King et al., 2019b; King et al., 2019c; Lokmer and Wegner, 2015). The consistent changes of several bacterial taxa across body compartments might suggest a coordinated community shift, which could potentially be explored as a marker for the onset of dysbiosis. Since such specific associations will also depend on the environmental conditions, further studies are needed to assess the robustness of such associations across heterogenous environments and a wider range of molluscan hosts and diseases. In the context of *Marteilia* infection, other taxa identified included Rickettsia-like, *Borrelia*, or *Hepatoplasma* strains, which have been found to dominate the microbiomes of infected Sydney rock oysters (Green and Barnes, 2010; Nguyen et al., 2021). However, these taxa were not observed in our dataset, further confirming that indicator species associated with infection, even among closely related parasites, can show limited overlap between host species from different sites, and thus only capture a momentary glimpse of the interaction.

Most indicator relative abundances in *Bonamia*-infected individuals also showed an increase, especially in the hemolymph and gill tissue, further suggesting a potential link between infection site and associated microbiota (Fig. 2). However, the taxa correlating with *Bonamia* infection largely differed from those identified in *Marteilia* infections. The most prominent indicators positively associated with *Bonamia* infection included ASV835 (*Acanthopleuribacter*), ASV1703 (SAR324) and ASV904, ASV1231 (*Motiliproteus*). Again, the high concentrations of ASV835 (*Acanthopleuribacter*), ASV1231

(*Motiliproteus*) and ASV1703 (SAR324) in gills, hemolymph and pallial fluid might reflect the tropism of *Bonamia*. The type strain of *Acanthopleuribacter* was isolated from another mollusk, the chiton *Acanthopleura japonica* (Fukunaga et al., 2008). This indicates that this taxon might be closely associated with mollusks, but it has not been connected with parasite infection or disease thus far. Similarly, *Motiliproteus* is a genus of marine bacteria, and some strains have been isolated from corals (Wang et al., 2018), but they have not been associated with disease in oysters. ASV1231 is particularly interesting in this context because it was one of the few taxa that showed opposing relative abundance patterns in the hemolymph. *O. edulis* infected with *M. refringens* had significantly higher relative abundances of ASV1231, while infection with *B. ostreae* correlated with a significant reduction when compared to the control (Fig. 2). Such taxa with opposite abundance patterns when infected by different pathogens could be promising candidates for differentiating between infection risks. The presence of indicator taxa will rather help to identify conditions that can promote disease, but cannot replace the direct monitoring of infection states with other methods (e.g. qPCR as applied here).

SAR324 is a ubiquitous *Deltaproteobacterium* described across the whole water column. It exhibits a remarkable genomic and metabolic diversity depending on the depths of isolation (Boeuf et al., 2021). This metabolic flexibility could indicate that a host-associated lifestyle is also possible. Alternatively, its high relative abundance in body compartments directly in contact with the water column could be an indirect effect. For example, if *Bonamia* infection modifies filtration rates or reduces the relative abundance of established microbiota, transient strains taken up from the environment can be amplified.

A similar indirect enrichment in environmental strains was observed in all body compartments of *M. gigas* infected with OsHV-1, where several cyanobacterial Chloroplast-ASVs were identified as indicator taxa positively associated with infection (Fig. 4). In contrast, *M. gigas* from OsHV-1 resistant families showed a higher relative abundance of Cyanobacteria when exposed to infectious conditions (Clerissi et

al., 2020a). While parasitic algae have been described in blue mussels (Rodriguez et al., 2008), the presence of phototrophic organisms does not necessarily imply symbiotic relationships with a host, since the increased relative abundance of cyanobacteria or algae could be interpreted as increased uptake rates or a depletion of persistent microbiota. However, their direct functional association to oyster microbiota remains to be investigated.

Indicator taxa positively associated with OsHV-1 infection included two ASVs classified as *Helicobacteriaceae* (Fig. 4). *Helicobacteraceae* are a regular part of oyster microbiota and can be the dominant taxon in the coelom of starfish, demonstrating its close association with invertebrate hosts (Nakagawa et al., 2017). However, in general, *Helicobacteraceae* taxa have not been associated with disease.

The role of microbiota in OsHV-1 infection of *M. gigas* has received more attention in general (Clerissi et al., 2020a; de Lorgeril et al., 2018; Delisle et al., 2022; King et al., 2019a), and the common set of taxa correlated with the infection included *Vibrio*, *Arcobacter*, *Mycoplasma*. However, in our study, we only identified one of these as an indicator taxon for OsHV-1 infection in *M. gigas* (ASV4: Mycoplasma). It is important to note that most of these previous studies investigated the microbiome response during phases of acute disease with high viral loads compared to the low virus loads we found in our samples. Considering temporal variation along infection cycles in acute (OsHV-1) and chronic infections (*B. ostreae, M. refringens*) will therefore be crucial to validate indicator taxa and distinguish them from opportunistic organisms that benefit from infection.

4.3 Conclusion

By simultaneously investigating prokaryotic and eukaryotic microbiota of two oyster species infected by three distinct pathogens, we demonstrated that bacterial microbiota contain more information regarding infection states than eukaryotic microbiota. Different classes of microbiota are frequently

investigated in environmental DNA (eDNA) samples (Sunagawa et al., 2015), but they are rarely considered simultaneously to characterize microbiota of the same host individual, with few exceptions (Dupont et al., 2020). This is also true for studies on bivalve diseases relevant for aquaculture, where the eukaryotic microbiota response to infectious conditions is rarely investigated (Dupont et al., 2020), despite the potential connection in animals with open circulatory systems and rich protist diversity like mollusks (Clerissi et al., 2020b). In contrast, many studies have focused on the role of bacterial microbiota (Paillard et al., 2022), and our results suggest that these studies have indeed investigated the more relevant microbiota compartment.

Previous studies on bacterial microbiomes often concentrated on the structural properties of the microbiota, such as within and between individual diversity, and then discussed the most common or core taxa. This approach may introduce potential bias toward taxa with low information content (common in many individuals) and overlook rarer microbial consortia with higher information content. The random forest classification approach employed in this study was the most powerful method to differentiate between infection states, potentially reducing such bias and enabling a more comprehensive identification of informative indicator taxa. Artificial intelligence (AI) and machine learning algorithms are gaining popularity and have demonstrated superiority over other approaches in studying microbiota (Statnikov et al., 2013). However, further research is needed to explore the advantages and disadvantages of this approach in identifying meaningful indicator taxa for infection and disease, as well as their application in an aquaculture setting. The next steps should also address the role of environmental variation across space and time to allow the inference of general patterns. While our pooling of samples from different time points averages out microbiome variation over time to a certain degree, the identity of indicator taxa certainly harbors an environmental component, which should be quantified by future studies.

Furthermore, our objective was to describe differences of pro- and eukaryotic microbiota in relation to infection by different classes of disease under natural conditions. Therefore, our data is solely correlational, and we cannot establish causation. Nonetheless, some of the observed patterns, which reflect the tropism of infection, suggest that infection may indeed be the cause for the coordinated changes observed in several indicator ASVs (e.g., the highest relative abundances in the digestive gland with spill-over into other body compartments in *Marteilia* infections). To validate the general applicability or common features of indicator taxa and advance the study of the microbiota-host-disease interface, further studies encompassing a broader environmental background and experimental verification through controlled infection or microbiota manipulation experiments in commercial aquaculture are required.

5 Acknowledgements

Declarations

Ethical Approval

All experiments were performed according to European animal welfare legislation.

Author contributions

KMW, BM, LG, MS MAT and IA conceptualized the study. BM, MS, CL, DT, OG, MAT, IA collected and processed samples, MS and KMW performed molecular analyses and sequencing. KMW analysed the data and wrote the first version of the manuscript. All authors contributed to the writing and editing of the final manuscript.

References

Aceveses, A.K., Johnson, P., Bullard, S.A., Lafrentz, S., Arias, C.R., 2018. Description and characterization of the digestive gland microbiome in the freshwater mussel Villosa nebulosa (Bivalvia: Unionidae),. Journal of Molluscan Studies 84(3), 240-246. https://doi.org/10.1093/mollus/eyy014

Arzul, I., Corbeil, S., Morga, B., Renault, T., 2017. Viruses infecting marine molluscs. Journal of Invertebrate Pathology 147, 118-135. https://doi.org/10.1016/j.jip.2017.01.009

Arzul, I., Miossec, L., Blanchet, E., Garcia, C., Francois, C., Joly, J.P., 2006. *Bonamia ostreae* and *Ostrea edulis*: A Stable Host-Parasite System in France? , 11th International Symposium on Veterinary Epidemiology and Economics. Cairns, Queensland, Australia.

Arzul, I., Nicolas, J.L., Davison, A.J., Renault, T., 2001. French scallops: A new host for ostreid herpesvirus-1. Virology 290(2), 342-349. https://doi.org/10.1006/viro.2001.1186

Bai, C.-M., Rosani, U., Zhang, X., Xin, L.-S., Bortoletto, E., Wegner, K.M., Wang, C.-M., 2021. Viral Decoys: The Only Two Herpesviruses Infecting Invertebrates Evolved Different Transcriptional Strategies to Deflect Post-Transcriptional Editing. Viruses 13(10), 1971. https://doi.org/10.3390/v13101971

Bass, D., Stentiford, G.D., Wang, H.C., Koskella, B., Tyler, C.R., 2019. The Pathobiome in Animal and Plant Diseases. Trends Ecol Evol 34(11), 996-1008. https://doi.org/10.1016/j.tree.2019.07.012

Boeuf, D., Eppley, J.M., Mende, D.R., Malmstrom, R.R., Woyke, T., DeLong, E.F., 2021. Metapangenomics reveals depth-dependent shifts in metabolic potential for the ubiquitous marine bacterial SAR324 lineage. Microbiome 9(1), 172. https://doi.org/10.1186/s40168-021-01119-5

Broadhurst, D.I., Kell, D.B., 2006. Statistical strategies for avoiding false discoveries in metabolomics and related experiments. Metabolomics 2(4), 171-196. https://doi.org/10.1007/s11306-006-0037-z

Callahan, B.J., McMurdie, P.J., Rosen, M.J., Han, A.W., Johnson, A.J.A., Holmes, S.P., 2016. DADA2: High-resolution sample inference from Illumina amplicon data. Nature Methods 13(7), 581-583. https://doi.org/10.1038/nmeth.3869

Canier, L., Dubreuil, C., Noyer, M., Serpin, D., Chollet, B., Garcia, C., Arzul, I., 2020. A new multiplex real-time PCR assay to improve the diagnosis of shellfish regulated parasites of the genus Marteilia and Bonamia. Prev. Vet. Med. 183. https://doi.org/10.1016/j.prevetmed.2020.105126

Chabe, M., Lokmer, A., Segurel, L., 2017. Gut Protozoa: Friends or Foes of the Human Gut Microbiota? Trends in Parasitology 33(12), 925-934. https://doi.org/10.1016/j.pt.2017.08.005

Clerissi, C., de Lorgeril, J., Petton, B., Lucasson, A., Escoubas, J.M., Gueguen, Y., Degremont, L., Mitta, G., Toulza, E., 2020a. Microbiota Composition and Evenness Predict Survival Rate of Oysters Confronted to Pacific Oyster Mortality Syndrome. Frontiers in microbiology 11, 311. https://doi.org/10.3389/fmicb.2020.00311

Clerissi, C., Guillou, L., Escoubas, J.M., Toulza, E., 2020b. Unveiling protist diversity associated with the Pacific oyster Crassostrea gigas using blocking and excluding primers. BMC Microbiol 20(1), 193. https://doi.org/10.1186/s12866-020-01860-1

Comps, M., Tigé, G., Grizel, H., 1980. Etude ultrastructurale d'un protiste parasite de l'huître *Ostrea edulis* L. Acad. Sc. Paris, Sér. D 290, 383-385.

de Lorgeril, J., Lucasson, A., Petton, B., Toulza, E., Montagnani, C., Clerissi, C., Vidal-Dupiol, J., Chaparro, C., Galinier, R., Escoubas, J.M., Haffner, P., Degremont, L., Charriere, G.M., Lafont, M., Delort, A., Vergnes, A., Chiarello, M., Faury, N., Rubio, T., Leroy, M.A., Perignon, A., Regler, D., Morga, B., Alunno-Bruscia, M., Boudry, P., Le Roux, F., Destoumieux-Garzomicronn, D., Gueguen, Y., Mitta, G., 2018. Immune-suppression by OsHV-1 viral infection causes fatal bacteraemia in Pacific oysters. Nat Commun 9(1), 4215. https://doi.org/10.1038/s41467-018-06659-3

Delisle, L., Laroche, O., Hilton, Z., Burguin, J.-F., Rolton, A., Berry, J., Pochon, X., Boudry, P., Vignier, J., 2022. Understanding the Dynamic of POMS Infection and the Role of Microbiota Composition in the Survival of Pacific Oysters, Crassostrea gigas. Microbiology Spectrum 10(6), e01959-01922. https://doi.org/doi:10.1128/spectrum.01959-22

Desriac, F., Le Chevalier, P., Brillet, B., Leguerinel, I., Thuillier, B., Paillard, C., Fleury, Y., 2014. Exploring the hologenome concept in marine bivalvia: haemolymph microbiota as a pertinent source of probiotics for aquaculture. FEMS microbiology letters 350(1), 107-116. https://doi.org/10.1111/1574-6968.12308

Dittmann, K.K., Sonnenschein, E.C., Egan, S., Gram, L., Bentzon-Tilia, M., 2019. Impact of Phaeobacter inhibens on marine eukaryote-associated microbial communities. Environ Microbiol Rep 11(3), 401-413. https://doi.org/10.1111/1758-2229.12698

Dupont, S., Lokmer, A., Corre, E., Auguet, J.C., Petton, B., Toulza, E., Montagnani, C., Tanguy, G., Pecqueur, D., Salmeron, C., Guillou, L., Desnues, C., La Scola, B., Bou Khalil, J., de Lorgeril, J., Mitta, G., Gueguen, Y., Escoubas, J.M., 2020. Oyster hemolymph is a complex and dynamic ecosystem hosting bacteria, protists and viruses. Animal Microbiome 2(1). https://doi.org/10.1186/s42523-020-00032-w

Esser, D., Lange, J., Marinos, G., Sieber, M., Best, L., Prasse, D., Bathia, J., Ruhlemann, M.C., Boersch, K., Jaspers, C., Sommer, F., 2019. Functions of the Microbiota for the Physiology of Animal Metaorganisms. J Innate Immun 11(5), 393-404. https://doi.org/10.1159/000495115

eurl-mollusc.eu, 2023. OsHV-1 detection and quantification by Real Time Polymerase Chain Reaction. https://www.eurl-mollusc.eu/content/download/42545/578238/file/OsHV-1+RTPCR_1.pdf?version=1.

Even, G., Lokmer, A., Rodrigues, J., Audebert, C., Viscogliosi, E., Segurel, L., Chabe, M., 2021. Changes in the Human Gut Microbiota Associated With Colonization by Blastocystis sp. and Entamoeba spp. in Non-Industrialized Populations. Frontiers in Cellular and Infection Microbiology 11. https://doi.org/10.3389/fcimb.2021.533528

Fukunaga, Y., Kurahashi, M., Yanagi, K., Yokota, A., Harayama, S., 2008. Acanthopleuribacter pedis gen. nov., sp. nov., a marine bacterium isolated from a chiton, and description of Acanthopleuribacteraceae fam. nov., Acanthopleuribacterales ord. nov., Holophagaceae fam. nov., Holophagales ord. nov. and Holophagae classis nov. in the phylum 'Acidobacteria'. Int J Syst Evol Microbiol 58(Pt 11), 2597-2601. https://doi.org/10.1099/ijs.0.65589-0

Green, T.J., Barnes, A.C., 2010. Bacterial diversity of the digestive gland of Sydney rock oysters, Saccostrea glomerata infected with the paramyxean parasite, Marteilia sydneyi. J Appl Microbiol 109(2), 613-622. https://doi.org/10.1111/j.1365-2672.2010.04687.x

Grizel, H., 1979. MARTEILIA-REFRINGENS AND OYSTER DISEASE - RECENT OBSERVATIONS. Marine Fisheries Review 41(1-2), 38-39.

Holmes, J.C., 1973. Site selection by parasitic helminths - interspecific interactions, site segregation, and their importance to development of helminth communities. Canadian Journal of Zoology 51(3), 333-347. https://doi.org/10.1139/z73-047

Kesarcodi-Watson, A., Miner, P., Nicolas, J.-L., Robert, R., 2012. Protective effect of four potential probiotics against pathogen-challenge of the larvae of three bivalves: Pacific oyster (Crassostrea gigas), flat oyster (Ostrea edulis) and scallop (Pecten maximus). Aquaculture 344-349, 29-34. https://doi.org/10.1016/j.aquaculture.2012.02.029

King, W.L., Jenkins, C., Go, J., Siboni, N., Seymour, J.R., Labbate, M., 2019a. Characterisation of the Pacific Oyster Microbiome During a Summer Mortality Event. Microbial Ecology 77(2), 502-512. https://doi.org/10.1007/s00248-018-1226-9

King, W.L., Jenkins, C., Seymour, J.R., Labbate, M., 2019b. Oyster disease in a changing environment: Decrypting the link between pathogen, microbiome and environment. Marine Environmental Research 143, 124-140. https://doi.org/10.1016/j.marenvres.2018.11.007

King, W.L., Siboni, N., Williams, N.L.R., Kahlke, T., Nguyen, K.V., Jenkins, C., Dove, M., O'Connor, W., Seymour, J.R., Labbate, M., 2019c. Variability in the Composition of Pacific Oyster Microbiomes Across Oyster Families Exhibiting Different Levels of Susceptibility to OsHV-1 mu var Disease. Frontiers in microbiology 10. https://doi.org/10.3389/fmicb.2019.00473

Le Roux, F., Wegner, K.M., Polz, M.F., 2016. Oysters and Vibrios as a Model for Disease Dynamics in Wild Animals. Trends Microbiol 24(7), 568-580. https://doi.org/10.1016/j.tim.2016.03.006

Lokmer, A., Goedknegt, M.A., Thieltges, D.W., Fiorentino, D., Kuenzel, S., Baines, J.F., Wegner, K.M., 2016. Spatial and Temporal Dynamics of Pacific Oyster Hemolymph Microbiota across Multiple Scales. Frontiers in microbiology 7, 1367. https://doi.org/10.3389/fmicb.2016.01367

Lokmer, A., Kuenzel, S., Baines, J., Wegner, K.M., 2016. The Role of Tissue-specific Microbiota in Initial Establishment Success of Pacific oysters. Environmental Microbiology 18(3), 970-987. https://doi.org/10.1111/1462-2920.13163

Lokmer, A., Wegner, K.M., 2015. Hemolymph microbiome of Pacific oysters in response to temperature, temperature stress and infection. ISME Journal 9, 670-682. https://doi.org/10.1038/ismej.2014.160

Nakagawa, S., Saito, H., Tame, A., Hirai, M., Yamaguchi, H., Sunata, T., Aida, M., Muto, H., Sawayama, S., Takaki, Y., 2017. Microbiota in the coelomic fluid of two common coastal starfish species and characterization of an abundant Helicobacter-related taxon. Sci Rep 7(1), 8764. https://doi.org/10.1038/s41598-017-09355-2

Nguyen, V.K., King, W.L., Siboni, N., Mahbub, K.R., Rahman, M.H., Jenkins, C., Dove, M., O'Connor, W., Seymour, J.R., Labbate, M., 2021. Dynamics of the Sydney rock oyster microbiota before and during a QX disease event. Aquaculture 541. https://doi.org/10.1016/j.aquaculture.2021.736821

Offret, C., Paulino, S., Gauthier, O., Chateau, K., Bidault, A., Corporeau, C., Miner, P., Petton, B., Pernet, F., Fabioux, C., Paillard, C., Le Blay, G., 2020. The marine intertidal zone shapes oyster and clam digestive bacterial microbiota. Fems Microbiology Ecology 96(8). https://doi.org/10.1093/femsec/fiaa078

Paillard, C., Gueguen, Y., Wegner, K.M., Bass, D., Pallavicini, A., Vezzulli, L., Arzul, I., 2022. Recent advances in bivalve-microbiota interactions for disease prevention in aquaculture. Curr Opin Biotechnol 73, 225-232. https://doi.org/10.1016/j.copbio.2021.07.026

Pichot, Y., Comps, M., Tigé, G., Grizel, H., Rabouin, M.A., 1979. Recherches sur Bonamia ostreae gen. n., sp. n., parasite nouveau de l'huitre plate Ostrea edulis L. Rev. Trav. Inst. Peches Marit. 43, 131-140.

Pierce, M.L., Ward, J.E., 2019. Gut Microbiomes of the Eastern Oyster (Crassostrea virginica) and the Blue Mussel (Mytilus edulis): Temporal Variation and the Influence of Marine Aggregate-Associated Microbial Communities. Msphere 4(6). https://doi.org/10.1128/mSphere.00730-19

Pimentel, Z.T., Dufault-Thompson, K., Russo, K.T., Scro, A.K., Smolowitz, R.M., Gomez-Chiarri, M., Zhang, Y., 2021. Microbiome Analysis Reveals Diversity and Function of Mollicutes Associated with the Eastern Oyster, Crassostrea virginica. mSphere 6(3). https://doi.org/10.1128/mSphere.00227-21

Pira, H., Risdian, C., Musken, M., Schupp, P.J., Wink, J., 2022. Photobacterium arenosum WH24, Isolated from the Gill of Pacific Oyster Crassostrea gigas from the North Sea of Germany: Co-cultivation and Prediction of Virulence. Curr Microbiol 79(8), 219. https://doi.org/10.1007/s00284-022-02909-2

Portet, A., Toulza, E., Lokmer, A., Huot, C., Duval, D., Galinier, R., Gourbal, B., 2021. Experimental Infection of the Biomphalaria glabrata Vector Snail by Schistosoma mansoni Parasites Drives

Snail Microbiota Dysbiosis. Microorganisms 9(5).
https://doi.org/10.3390/microorganisms9051084

[dataset] Pouvreau, S., Cochet, H., Bargat, F., Petton, S., Le Roy, V., Guillet, T., Potet, M., 2021. Current distribution of the residual flat oysters beds (*Ostrea edulis*) along the west coast of France. SEANOE. https://doi.org/10.17882/79821

Pouvreau, S., Lapègue, S., Arzul, I., Boudry, P., 2023. Fifty years of research to counter the decline of the European flat oyster (Ostrea edulis): a review of French achievements and prospects for the restoration of remaining beds and revival of aquaculture production. Aquatic Living Resources 36. https://doi.org/10.1051/alr/2023006

Ray, N.E., Fulweiler, R.W., 2020. Meta-analysis of oyster impacts on coastal biogeochemistry. Nature Sustainability 4(3), 261-269. https://doi.org/10.1038/s41893-020-00644-9

Rodriguez, F., Feist, S.W., Guillou, L., Harkestad, L.S., Bateman, K., Renault, T., Mortensen, S., 2008. Phylogenetic and morphological characterisation of the green algae infesting blue mussel Mytilus edulis in the North and South Atlantic oceans. Dis Aquat Organ 81(3), 231-240. https://doi.org/10.3354/dao01956

Rueckert, S., Wakeman, K.C., Jenke-Kodama, H., Leander, B.S., 2015. Molecular systematics of marine gregarine apicomplexans from Pacific tunicates, with descriptions of five novel species of Lankesteria. Int J Syst Evol Microbiol 65(8), 2598-2614. https://doi.org/10.1099/ijs.0.000300

Segarra, A., Pepin, J.F., Arzul, I., Morga, B., Faury, N., Renault, T., 2010. Detection and description of a particular Ostreid herpesvirus 1 genotype associated with massive mortality outbreaks of Pacific oysters, Crassostrea gigas, in France in 2008. Virus Research 153(1), 92-99. https://doi.org/10.1016/j.virusres.2010.07.011

Słodkowicz-Kowalska, A., Majewska, A.C., Rzymski, P., Skrzypczak, L., Werner, A., 2015. Human waterborne protozoan parasites in freshwater bivalves (*Anodonta anatina* and *Unio tumidus*) as potential indicators of fecal pollution in urban reservoir. Linmologica 51, 32-36. https://doi.org/10.1016/j.limno.2014.12.001.

Statnikov, A., Henaff, M., Narendra, V., Konganti, K., Li, Z.G., Yang, L.Y., Pei, Z.H., Blaser, M.J., Aliferis, C.F., Alekseyenko, A.V., 2013. A comprehensive evaluation of multicategory classification methods for microbiomic data. Microbiome 1. https://doi.org/10.1186/2049-2618-1-11

Strittmatter, M., 2023a. PCR for metabarcoding of the eukaryotic microbiome of two oyster species, Crassostrea gigas and Ostrea edulis. https://doi.org/dx.doi.org/10.17504/protocols.io.5k6g4ze

Strittmatter, M., 2023b. Simultanuous DNA and RNA extraction from various tissues of the two oyster species, Crassostrea gigas and Ostrea edulis, for metabarcoding. protocols.io. https://doi.org/dx.doi.org/10.17504/protocols.io.22aggae

Sunagawa, S., Coelho, L.P., Chaffron, S., Kultima, J.R., Labadie, K., Salazar, G., Djahanschiri, B., Zeller, G., Mende, D.R., Alberti, A., Cornejo-Castillo, F.M., Costea, P.I., Cruaud, C., d'Ovidio, F., Engelen, S., Ferrera, I., Gasol, J.M., Guidi, L., Hildebrand, F., Kokoszka, F., Lepoivre, C., Lima-Mendez, G., Poulain, J., Poulos, B.T., Royo-Llonch, M., Sarmento, H., Vieira-Silva, S., Dimier, C., Picheral, M., Searson, S., Kandels-Lewis, S., Bowler, C., Vargas, C.d., Gorsky, G., Grimsley, N., Hingamp, P., Iudicone, D., Jaillon, O., Not, F., Ogata, H., Pesant, S., Speich, S., Stemmann, L., Sullivan, M.B., Weissenbach, J., Wincker, P., Karsenti, E., Raes, J., Acinas, S.G., Bork, P., Boss, E., Bowler, C., Follows, M., Karp-Boss, L., Krzic, U., Reynaud, E.G., Sardet, C., Sieracki, M., Velayoudon, D., 2015. Structure and function of the global ocean microbiome. Science 348(6237), 1261359. https://doi.org/doi:10.1126/science.1261359

Wang, G., Xu, S., Su, H., Chen, B., Huang, W., Liang, J., Wang, Y., Yu, K., 2018. Motiliproteus coralliicola sp. nov., a bacterium isolated from coral. Int J Syst Evol Microbiol 68(10), 3292-3295. https://doi.org/10.1099/ijsem.0.002984

Wegner, K.M., Volkenborn, N., Peter, H., Eiler, A., 2013. Disturbance induced decoupling between host genetics and composition of the associated microbiome. BMC Microbiology 13, 252.

Whitman, W.B., Coleman, D.C., Wiebe, W.J., 1998. Prokaryotes: The unseen majority. Proceedings of the National Academy of Sciences 95, 6578-6583.

Author Statement

With the submission of this manuscript, I would like to confirm that the above-mentioned manuscript has not been published elsewhere, accepted for publication elsewhere or under editorial review for publication elsewhere. No AI tools were used to write the manuscript, and all co-authors approved of the current version. KMW, BM, LG, MS MAT and IA conceptualized the study. BM, MS, CL, DT, OG, MAT, IA collected and processed samples, MS and KMW performed molecular analyses and sequencing. KMW analysed the data and wrote the first version of the manuscript. All authors contributed to the writing and editing of the final manuscript.

Declaration of interests

☒The authors declare that they have no known competing financial interests or personal relationships that could have appeared to influence the work reported in this paper.

☐The authors declare the following financial interests/personal relationships which may be considered as potential competing interests:

Highlights

- Bacterial microbiota are more strongly associated to infection states than protist microbiota
- Only few indicator taxa are needed to maximize differentiation between infection states
- The higher information content of only a few bacterial taxa needed to identify disease states was found across three pathogens and two commercially important oyster hosts